A microarray to measure repair of damaged plasmids by cell lysates

J.-F. Millau,†[a] A.-L. Raffin,†[a] S. Caillat,[a] C. Claudet,[a] G. Arras,[b] N. Ugolin,[b] T. Douki,[a] J.-L. Ravanat,[a] J. Breton,[a] T. Oddos,[c] C. Dumontet,[e] A. Sarasin,[d] S. Chevillard,[b] A. Favier[a] and S. Sauvaigo[a]

Received 18th April 2008, Accepted 26th June 2008
First published as an Advance Article on the web 28th August 2008
DOI: 10.1039/b806634e

DNA repair mechanisms constitute major defences against agents that cause cancer, degenerative disease and aging. Different repair systems cooperate to maintain the integrity of genetic information. Investigations of DNA repair involvement in human pathology require an efficient tool that takes into account the variety and complexity of repair systems. We have developed a highly sensitive damaged plasmid microarray to quantify cell lysate excision/synthesis (ES) capacities using small amounts of proteins. This microsystem is based on efficient immobilization and conservation on hydrogel coated glass slides of plasmid DNA damaged with a panel of genotoxic agents. Fluorescent signals are generated from incorporation of labelled dNTPs by DNA excision-repair synthesis mechanisms at plasmid sites. Highly precise DNA repair phenotypes *i.e.* simultaneous quantitative measures of ES capacities toward seven lesions repaired by distinct repair pathways, are obtained. Applied to the characterization of xeroderma pigmentosum (XP) cells at basal level and in response to a low dose of UVB irradiation, the assay showed the multifunctional role of different XP proteins in cell protection against all types of damage. On the other hand, measurement of the ES of peripheral blood mononuclear cells from six donors revealed significant diversity between individuals. Our results illustrate the power of such a parallelized approach with high potential for several applications including the discovery of new cancer biomarkers and the screening of chemical agents modulating DNA repair systems.

Introduction

Research on DNA repair never ceased to gain interest since the discovery in 1964 of the nucleotide excision repair (NER) mechanism for the repair of UV-induced damage[1] and of the link between repair defects and the skin cancer-prone syndrome xeroderma pigmentosum (XP).[2] These discoveries emphasized the critical importance of maintaining DNA integrity and genome stability and led to the identification of other DNA repair systems and their implication in aging,[3,4] cancer,[5] genetic diseases[6] and drug resistance.[7] Six basic repair systems are identified in humans. Among them, typically, NER processes bulky damage able to distort the DNA helix,[8] base excision repair (BER) is devoted to the repair of small base lesions.[9]

These specialized repair pathways have evolved to cover most of the genotoxic events. However, recent evidences suggest that they cross-talk and partly overlap.[10–12] It is therefore important to investigate DNA repair activities as a network of mechanisms to understand how the different cellular effectors act or interact. However, commonly used methods that permit such a characterization, including the comet assay,[13] the host cell reactivation assay[14] and cleavage assays on synthetic oligonucleotides,[15] present a low throughput and are dedicated to DNA repair phenotyping of a single lesion. Therefore, we designed a miniaturized and parallelized *in vitro* cell free assay that allows us to investigate simultaneously NER and BER functionality in cell extracts. These two repair processes involve first excision of the damaged DNA followed by a subsequent DNA synthesis using the resulting single-stranded gap as a template. Our assay takes advantage of this synthesis step to incorporate fluorescently labelled nucleotides into immobilized damaged plasmids. Distinct plasmids bearing different types of lesions were created and spotted onto a gel-coated surface. The microarray format allows simultaneous measurement of the excision/synthesis (ES) activity of seven families of DNA lesions by nuclear extracts.

In this article we present this new technological approach, the principle and conception of the assay and demonstrate its validity by biochemical characterizations. We further validate the assay by phenotyping the ES activities of XP repair-deficient cell lines exposed or not to UVB irradiation. We also applied it to the repair phenotyping of peripheral blood mononuclear cells (PBMCs) isolated from different donors. We show that this assay is faster than current assays, is easy to perform, gives precise and

[a]*Laboratoire des Lésions des Acides Nucléiques, LCIB (UMR-E 3 CEA-UJF), INAC, CEA Grenoble, 38054, Grenoble cedex 9, France*
[b]*Laboratoire de Cancérologie Expérimentale, CEA-DSV-DRR, 18 route du panorama, BP 6, 92265, Fontenay aux Roses cedex, France*
[c]*Johnson & Johnson Consumer Europe, Campus de Maigremont, 27100, Val de Reuil, France*
[d]*CNRS FRE 2939, Institut Gustave Roussy and Université Paris-Sud, 39 rue Camille Desmoulins, 94805, Villejuif, France*
[e]*Inserm, U590, Lyon, F-69008, France, Université Lyon, LCMT, Lyon, F-69003, France*
† These authors contributed equally to this project and should be considered co-first authors.

quantitative phenotypes with a high level of information and can be applied without restriction on cell type.

Materials and methods

Plasmid preparation

pBluescript plasmid (Stratagene) was produced by standard methods, purified using the Plasmid Purification Kit Maxi (Qiagen) and precipitated in isopropanol/Na acetate. The pellet was washed in ice-cold 70% ethanol and, after drying, re-suspended at 1 mg mL^{-1} in 100 µL PBS (Interchim) and stored at –80 °C.

Creation of DNA lesions on plasmids

Preparation of pCPD-64 plasmid: to minimize possible formation of oxidative damage due to the natural presence of O_2 in the aqueous solution, UVC irradiation was performed using frozen plasmid solution. Frozen drops (25 µL) of 40 µg mL^{-1} plasmid solution in PBS were exposed to UVC radiation emitted by a VL 15-C lamp (Bioblock Scientific). Irradiation dose was 0.3 J cm^{-2} during 2 min at 2.5 mW fluence rate, measured with VLX 3 W radiometer (Vilbert Lourmat) equipped with a 254 nm probe.

Preparation of pAbaS plasmid: Abasic sites were created by acidic treatment of the DNA at an elevated temperature. The plasmid DNA (100 µL at 1 mg mL^{-1} in PBS + 0.2 M KCl) was incubated with 5 µL of 0.5 M sodium citrate pH 4.8 for 4 h at 70 °C.

Riboflavin photosensitization of p8oxo plasmid: 100 µL of 1 mg mL^{-1} plasmid in PBS and 10 µL of 400 mM riboflavin (Sigma, St. Louis, MO, USA) were placed in a vial and irradiated for 2 min with an 500 W halogen lamp at a distance of 10 cm. Water flow was placed between the sample and the lamp to keep the sample cold (15 °C).[16]

Preparation of pGlycol plasmid: 200 µL of 1 mg mL^{-1} plasmid was reacted with 20 µL 0.4 M $KMnO_4$ (Sigma, St. Louis, MO, USA) diluted in 0.4 M potassium phosphate and the reaction was carried out for 5 min at 4 °C.[17] After the addition of 5 µL of allyl alcohol (Sigma, St. Louis, MO, USA), the solution was further incubated for 30 min at 4 °C. After elimination of the precipitate by centrifugation at 10 000 rpm for 10 min at 4 °C, the DNA contained in the supernatant was purified on a NAP-10 column (Amersham, Little Chalfont, England), then washed with 1.5 mL of sodium phosphate 10 mM.

Preparation of pAlkB plasmid: 200 µL of plasmid at 1 mg mL^{-1} in PBS, 200 µL of 0.2 M carbonate/bicarbonate (CO_3/HCO) pH 9.2 (Sigma, St. Louis, MO, USA), 200 µL of tetrahydrofurane (Carlo EBRA, Milan Italy), 4 µL of 5.7 M *trans*,*trans*-2-4-decadienal (DDE) (Sigma, St. Louis, MO, USA), and 12 µL of 8.8 M H_2O_2 (Sigma, St. Louis, MO, USA) were mixed and incubated for 16 h at 50 °C in the dark.[18]

Preparation of pCisP plasmid: 150 µL of plasmid at 1 mg mL^{-1} in PBS and 1 µL of cis-diaminedichloro-platinium(II) (Aldrich, Milwaukee, USA) prepared at 15 mg mL^{-1} in DMSO were mixed and incubated in the dark for 2 h at 37 °C.[19]

Preparation of pPso plasmid: A solution composed of 150 µL of plasmid at 1 mg mL^{-1} in PBS and 20 µL of psoralen amine (Sigma, St. Louis, MO, USA) at 120 µM was irradiated with a T-15L UVA light (Bioblock Scientific, Illkirch, France). Irradiation was performed for 10 min at 1.48 J cm^{-2} measured with a VLX 3 W radiometer equipped with a 365 nm probe.[20]

Except for UVC irradiated plasmid, the supercoiled fraction of the treated plasmids was purified by sucrose density gradient centrifugation.[21] Fractions of treated plasmid (100 µL) were carefully layered on the top of the gradient and centrifuged for 17 h at 25 000 rpm at 4 °C. Fractions of 800 µL were carefully transferred from the top of the tube to microcentrifuge tubes and subsequently analysed by electrophoresis on 1% agarose gel in TAE 1X. Fractions containing less than 10% of relaxed and linear plasmids were pooled and the plasmids were precipitated by isopropanol as already described. Plasmids were suspended in PBS and kept frozen at –20 °C.

Just before spotting, the different damaged plasmids were diluted in PBS at a final concentration of 40 µg mL^{-1}. For each treated plasmid, 3 solutions of identical DNA concentrations but with different lesion frequencies were prepared (called A, B and C for dilutions $\frac{1}{2}$, $\frac{3}{4}$ and 1, respectively).

Quantification of the ratio of lesions per plasmid

An average of 0.5 AP sites/DNA molecules were obtained as judged by the amount of the conversion of closed circular DNA to open circular DNA after digestion by an excess of the *Escherichia coli* enzyme endonuclease III. For the quantification of other base lesions, plasmid DNA was digested and analyzed by HPLC-MS/MS (API3000 triple quadrupolar mass spectrometer, Perkin Elmer/SCIEX) as described[22] except for the content in 8-oxoGua that was determined using a series 1100 HPLC system (Agilent Technologies) associated with a coulometric electrochemical detector Coulochem II equipped with a 5011 cell (ESA).[23]

Damaged plasmid microarray fabrication

Plasmid microarrays were prepared on HydroGel™ slides (Perkin Elmer). Plasmid solutions were spotted using a SciFlexarrayer piezo arrayer (Scienion AG). Three drops of solution were deposited per spot, corresponding to 1.5 nL and 60 pg of plasmids. Typically, spot diameter was 250 µm. Six plasmid microarrays were prepared per HydroGel™ slide. The position of the spots on each microarray was randomly attributed. Batches of 23 slides were prepared per run. After preparation, spotted HydroGel™ slides were stored sealed at 4 °C, for at least five days, allowing plasmids to immobilize.

Cells

To validate the assay, we used SV40 immortalized human fibroblasts cell lines from repair-deficient patients (AS1WT (XPC), XP12ROSV (XPA)) and MRC5 as control fibroblasts, provided by A. Sarasin. GM16093 (XPC) and GM14930 (XPG) were purchased from Coriell Institute for Medical Research (Camden, USA). The cells were cultured in MEM medium (MRC5, AS1WT, XP12ROSV) or MEM Non Essential Amino Acid(GM16093) or DMEM medium (GM 14930) containing 10% SVF, 2 mM L-glutamine, 220 U mL^{-1} penicillin, 220 µg mL^{-1} streptomycin at 37 °C in a 5% CO_2 humidified atmosphere.

Cells were harvested during the exponential phase of growth at 70% confluence and stored frozen in liquid nitrogen in culture medium containing 10% DMSO.

MRC5, XPC (AS1WT) and XPA (XP12ROSV) cells were irradiated with an UVB source mostly emitting at 312 nm as already described[22] at the dose of 5 J m^{-2} measured by a VLX3W radiometer (Vilbert Lourmat, Marne la Vallée, France). Cells were collected 24 h after irradiation. Viability was assessed by MTT assay conducted 24 h after irradiation.[24] At this dose, it was 90 ± 4%, 63 ± 5% and 82 ± 8% for MRC5, XPC and XPA, respectively. Note that at higher doses, viability of XPA was lower than viability of the XPC cell line.

Circulating PBMCs were obtained by venipuncture of healthy donors with their informed consent. PBMCs were obtained by density gradient centrifugation (Ficoll-Hypaque, 20 min centrifugation at 1650 *g* at 20 °C). The PBMCs were then washed twice in cold PBS, centrifuged for 5 min at 400 *g* at 4 °C. Finally, the pellet was suspended in 1 mL of RPMI 1640 culture medium (Invitrogen) containing 10% DMSO and 10% SVF. PBMCs were then frozen in liquid nitrogen until processed for extract preparation.

Cell nuclear extracts

HeLa nuclear extracts, purchased in bulk quantities and stored in aliquots at –80 °C, came from CIL Biotech. Nuclear extracts from other cell types were prepared according to a protocol modified from Dignam *et al.*[25] Freshly harvested cells or thawed cells were washed twice in ice-cold PBS. The cell pellet (about 2×10^6 cells) was suspended in 1 mL of ice-cold buffer A (10 mM HEPES pH 7.9, 1.5 mM $MgCl_2$, 10 mM KCl, 0.02% Triton X-100, 0.5 mM DTT, 0.5 mM PMSF). After 20 min on ice, lysis was completed by vortexing the tube for 30 s. Cell lysis was controlled by trypan blue exclusion assay. Nuclei were recovered by centrifugation for 5 min at 5000 rpm at 4 °C and suspended in 25 µL of ice-cold buffer B (10 mM HEPES pH 7.9, 1.5 mM $MgCl_2$, 400 mM KCl, 0.2 mM EDTA, 25% glycerol, 0.5 mM DTT, complete-mini antiproteases (Roche) and 0.5 mM PMSF). Nuclear membranes were lysed for 20 min on ice and two cycles of freezing–thawing at –80 °C and 4 °C, respectively. The extracts were cleared by centrifugation for 10 min at 13 000 rpm at 4 °C. The supernatant was recovered and stored frozen in aliquots at –80 °C.

Protein concentration (typically 2.5 mg mL^{-1} for the fibroblasts) was determined using the BCA kit (Interchim). Protein concentration of extracts prepared from PBMCs was around 8.5 mg mL^{-1} (mean 8.51 ± 0.84; $n = 6$).

DNA excision/synthesis assay

The excision/synthesis assay was performed as described[26] with slight modifications. Standard 50 µL repair assay mix contained 10 µL of 5X ATG buffer (200 mM Hepes KOH pH 7.8, 35 mM $MgCl_2$, 2.5 mM DTT, 1.25 µM dATP, 1.25 µM dTTP, 1.25 µM dGTP, 17% glycerol, 50 mM phosphocreatine (Sigma), 10 mM EDTA, 250 µg mL^{-1} creatine phosphokinase, 0.5 mg mL^{-1} BSA) together with 1 mM ATP (Amersham), 1.25 µM dCTP-Cy5 or 1.25 µM dGTP-Cy5 and 1.25 µM dCTP-Cy3 (Amersham) when specified. Experiments with commercial HeLa nuclear extracts were performed at the final concentration of 2 mg mL^{-1} for optimized times. ATP experiments were conducted for 1 h at 30 °C. For the validation with XP cell lines, a final protein concentration of 0.2 mg mL^{-1} was used. The mean values of 2 experiments performed using 2 plasmid microarrays per condition and obtained after 2 h repair are displayed. Experiments on PBMCs extracts were conducted for 3 time points (30 min, 1 h and 2 h) at 30 °C using a final protein concentration of 0.5 mg mL^{-1} and 1 plasmid microarray per condition.

Custom designed adhesive microarray covers (Grace Bio-Labs) were set on each slide. The reaction chambers were filled with 20 µL of the repair mix and sealed with a coverslip. The repair assay was carried out at 30 °C for the indicated time in the dark. Microarray covers were then removed and the slides were washed in a slide holder for 2 × 3 min in PBS/Tween 0.05% and 2 × 3 min in MilliQ water. Water was removed from the slides by 3 min centrifugation at 700 rpm. The hydrogels were then dried for 5 min at 30 °C.

Microarray scanning and fluorescence quantification

Images were acquired at 635 nm and 532 nm wavelengths at 5 µm resolution using a Genepix 4200A scanner (Axon Instrument). Total spot fluorescence intensity was calculated using the Genepix Pro 5.1 software (Axon Instrument).

Data normalization

Each experiment was carried out as 3 counterparts (except when indicated). If there were no experimental errors, the three counterparts would have the same average, the same variance and would display between them a linear regression passing by 0 with a slope of 1. But whatever the precautions that have been taken, experimental fluctuations occurred. This led to more or less variations in the measurements of the three counterparts of a given experiment.

However, the average and the variance of an experiment can respectively be approximated by the average of the averages $\bar{X}_k = (\sum \bar{x}_l)/3$ and the average of the standard deviations $\bar{C}_k = (\sum C_l)/3$ of the three counterparts.

To minimize the errors made between the three counterparts, the first step consisted in centring around X_k and normalizing by σ_k each counterpart, such as

$$X_{i,k} = \left[\left(x_{k,i} - \overline{x_k}\right)/C_k\right]\left(\sum C_l\right)/3 + \left(\sum \overline{x_l}\right)/3$$

Thus, after centering and normalising, the three counterparts have the same average and the same standard deviation.

In a second step, for each combination (k, l) of two counterparts chosen among the three ones, a recursive linear regression was calculated.

In absence of a reference, for the regression line between two counterparts with a slope different from 1, it is impossible to determine on which counterpart the greatest error has been made. To estimate and minimize the errors made between the counterparts, reliability factors were calculated for each twin spot (i,i) of a combination (k, l) of two counterparts.

Let us consider, $g_{k,i} = X_{k,i}/\bar{X}_k$ and $g_{l,i} = X_{l,i}/\bar{X}_l$, a reliability factor $re_{k,l,i}$ was calculated for each twin spot (i,i) such as, if

$g_{k,i} > g_{l,i}$, then $re_{k,l,i} = g_{l,i}/g_{k,i}$, else $re_{k,l,i} = g_{k,i}/g_{l,i}$. This reliability factor informed about the experimental error between the ($X_{k,i}$, $X_{l,i}$) values of the twin spot (i,i) for counterparts k and l in function of the regression straight line. The $re_{k,l,i}$ factor allowed the calculation of the averages $\bar{X}_k = (\sum re_{k,l,i} X_{k,i})/\sum re_{k,l,i}$, the variances $C^2{}_k = (\sum re_{k,l,i} X^2{}_{k,i})/\sum re_{k,l,i} - \bar{X}^2{}_k)$ and the covariances $Covar_{k,l} = [\sum re_{k,l,i}(X_{k,i} - \bar{X}_k)(X_{l,i} - \bar{X}_l)]/\sum re_{k,l,i}$, which led to the weighted correlation factor $R = Covar_{k,l}/(\sigma_k \sigma_l)$ of the regression line between a combination (k, l) of counterparts. Several regression iterations were carried out and for each, the $re_{k,l,i}$ was recomputed. Each iteration was accompanied by a correction of the scatter plot ($X_{k,i}$, $X_{l,i}$) in order to set the regression straight to the line of slope 1. A threshold ranging between 0 and 0.4 and growing with a step of 0.01 at each iteration, was imposed on $re_{k,l,i}$, such as only the twin spot (i,i) of a combination (k, l) where $re_{k,l,i}$ is higher than the threshold was taken into account for the regression calculation. The iteration of the correlations stopped once the correlation factor reached a value higher than 0.95, or once more than 10% of the spots were rejected by the threshold. For each counterparts (k, l), the value $m_{k,l,i}$ of the twin spot (i,i) was calculated as $m_{k,l,i} = \sqrt{X^2_{k,i} + X^2_{l,i}}/\sqrt{2}$. After the regression calculation of all counterpart combinations, the final value of the spot i among all counterparts was calculated as the average of the $m_{k,l,i}$, weighted by the respective $re_{k,l,i}$, such as $\bar{M}_i = (\sum\sum re_{k,l,i} \cdot m_{k,l,i})/\sum\sum re_{k,l,i}$.

Data expression and analysis

A data colour map was drawn using Acuity 3.1 software (Axon Instrument). As can be observed in Fig. 3a it represented a convenient means to view all the data simultaneously (the 3 dilutions of each damaged plasmid for the 3 protein concentrations) whereas the curve presented in Fig. 3b displayed only the results obtained using damaged plasmid dilution C.

For the characterization of the DNA ES activities of PBMCs, total repair fluorescence intensity was calculated by addition of the fluorescence intensity of the data for each lesion at each plasmid dilution and after subtraction of the values of the control (Fig. 8a). The contribution of the repair activity toward each lesion was calculated as a percentage of this total fluorescence intensity (taken as 100% for each donor) (Fig. 8b).

Results

Repair assay principle

DNA excision synthesis was carried out by incubating cell-free extracts with closed-circular plasmid DNA containing specific base lesions.[27] However, to benefit from the microarray format, we immobilized on the same support a set of distinct plasmids bearing lesions repaired by BER and/or NER. Both repair pathways can be roughly broken down into 4 steps: recognition of the lesion, excision of the damaged base, gap-filling DNA synthesis and ligation.[28] The assay takes advantage of the DNA synthesis step to incorporate labelled nucleotides, either dCTP-Cy5 or dGTP-Cy5 and dCTP-Cy3, at the repaired lesion sites. The repair signal at each plasmid site was measured with a microarray scanner and expressed as an intensity of fluorescence.

Damaged plasmid microarray design and fabrication

A long-term stable support that could maintain the plasmid DNA in a closed-circular form and that allows high sensitivity was required. We first tested poly-L-lysine coated slides, known to strongly fix DNA. However, electrostatic interactions between the DNA and the cationic polymer led to rapid plasmid breakage upon drying and consequently to high non specific signal (data not shown). We chose commercially available HydroGel™ slides (Perkin Elmer). This hydrated 3D-polyacrylamide gel allows fixation of biomolecules by physical adsorption, shows low intrinsic fluorescence and preserves the closed-circular plasmid structure for more than 6 weeks at 4 °C. Moreover, this surface greatly improved the spot morphology and the sensitivity of the system (data not shown).

We created 7 different derivatives of the pBluescript (pControl) plasmid. pCPD-64 contained cyclobutane pyrimidine dimers (CPD) and 6–4 photoproducts (6-4PPs). pCisP contained cisplatin adducts, mainly G-G and G-A intra-strand crosslinks and G-G inter-strand crosslinks.[29] pPso contained T-T inter- and intra-strand crosslinks.[30] These lesions are typically repaired by NER. p8oxo contained 8-oxoGuanine (8-oxoGua),[16] pAlkB contained alkylated bases, especially ethenoguanine derivatives (EthGua),[31] pAbaS contained abasic (AP) sites and pGlycol contained thymine glycols (Tg) and to a lower extent cytosine glycols (Cg).[32] These latter lesions are typically repaired by BER. The number of lesions per plasmid was measured and adjusted to obtain balanced repair signals (Table 1).

Table 1 Ratio of the different lesion types per plasmid (3000 bp)

	6-4PPs[a]	CPDs[a]	Glycol[a]	8-oxoGua[a]	ε*Gua*[a]	ε*Ade*[a]	Cisplatin Intra-1,2-d(GpG)[a]	AP site[b]
pControl	0.0	0.0	0.0	0.2	0.0	0.0	nd	nd
pCPD-64	25.7	34.5	nd	0.1	nd	nd	nd	nd
p8oxo	nd	nd	0.0	3.7	nd	nd	nd	nd
pAlkB	nd	nd	0.3	0.2	10.9	0.0	nd	nd
pCisP	nd	nd	0.0	0.1	nd	nd	7.5	nd
pPso	0.0	0.0	0.0	0.2	nd	nd	nd	nd
pAbaS	nd	nd	nd	nd	nd	nd	nd	0.5
pGlycol	nd	nd	1.1	0.2	nd	nd	nd	nd

[a] The number of lesions was determined by HPLC coupled to tandem mass spectrometry. [b] The number of abasic sites was determined by exonuclease III digestion and gel electrophoresis assay. nd, not determined.

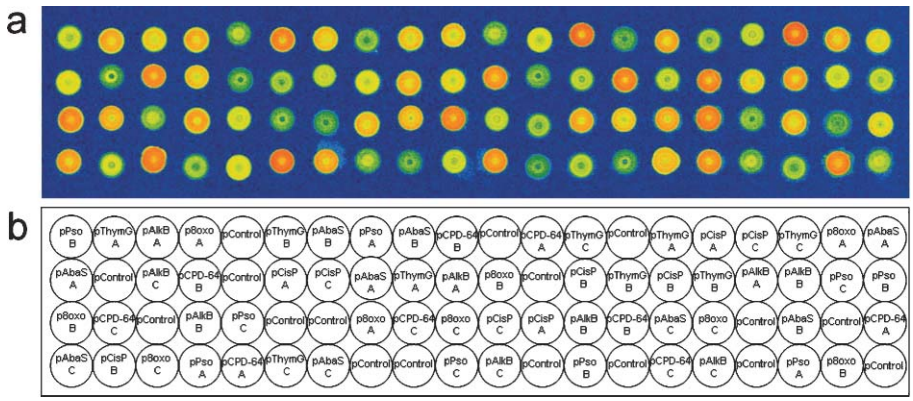

Fig. 1 Typical rainbow scale colorized image obtained after excision/synthesis reaction on the damaged plasmid microarray (a). The repair reaction was performed with HeLa nuclear extracts at 2 mg mL^{-1} for 3 h. The positions of the different plasmids were randomly attributed (b).

A piezoelectric arrayer was chosen over a contact-dispenser to avoid gel drying before spotting and gel deterioration during spotting. Each microarray contained 80 spots (3 dilutions of each lesion in triplicate and 17 control plasmid spots; Fig. 1).

Confocal microscopy visualization of the immobilized repaired plasmid

In order to investigate how plasmids were trapped into the hydrogel and where the DNA repair reaction occurred, we prepared a microarray with Cy3-labeled plasmid mixed with UVC-damaged plasmids. We then performed the repair reaction in the presence of dCTP-Cy5. Using the optical cross-sectioning capability of a confocal microscope and monitoring the Cy3 fluorescence, we imaged the immobilized plasmid into hydrogel. As shown on Fig. 2, spotted plasmids were located in the upper 8 μm of the hydrogel layer. Monitoring of the Cy5 fluorescence showed that the repair reaction occurred in the upper 3 μm of the gel layer.

Fig. 2 Reconstituted vertical cut of a spot in the gel using confocal laser scanning microscopy (magnification ×40). A stack of 50 sections (0.5 μm each) in the *z* axis was acquired from the surface of the gel to the inside, allowing spatial reconstitution of the spot. Repaired plasmid appeared in red superimposed to spotted plasmid that appeared in blue. Spotted plasmids stick into the upper 8 μm of the hydrogel layer. Repair reaction occurred in the upper 3 μm of the gel thickness.

Microarray quantification and normalisation

To quantify the fluorescent signal, we chose the total intensity of fluorescence which is the sum of fluorescence intensities of all the pixels contained in the area of interest (AOI) defined around each spot. Only pixels with intensity values greater than 2 times the standard deviation of the background (outside the AOI) were considered to be part of a spot. This strategy reduced the error linked to spot size (data not shown). Background signal was not subtracted as this feature was not allowed by the quantification software for total intensity fluorescence. However, this factor was negligible as hydrogel coating exhibited a very low and homogeneous background (Fig. 1). To minimize errors due to inter- and intra-slide variability, for each experimental point, triplicate microarrays distributed on three different slides were assayed (except where mentioned). The results were then normalized using recursive regressions performed by a software specifically developed for this purpose. During this process a reproducibility estimator was calculated for each spot and used to balance the fluorescence intensity.

Assessment of repair assay conditions

Commercial HeLa nuclear extracts were used to determine the optimal experimental conditions. We assessed the reproducibility of our test by performing two identical but independent repair experiments 27 days apart. A scatter plot of spot fluorescence intensities obtained from both experiments indicated a high reproducibility ($y = 1.0979x$, $R^2 = 0.9431$). We then conducted experiments using different extract concentrations and incubation times. For all the damaged plasmids, repair signal intensity increased with increasing protein concentration (Fig. 3), although only the repair of pCis and pPso gave a signal linearly correlated with the protein content.

The kinetics of DNA repair were established over a 4 h period using a protein concentration of 2 mg mL^{-1}. Fluorescence incorporation into the control plasmid remained very low. The shapes and slopes of the resulting curves were different for each lesion (Fig. 4). Interestingly, the highest repair rate was observed for lesions known to be handled by BER: glycols, 8-oxoGua, alkylated bases and AP sites. The slope of the repair curve of psoralen adducts started to increase only after 3 h, suggesting that initiation steps of the repair reaction were very slow for these adducts.

Requirement for ATP in the repair/synthesis process was then assessed. As expected, ES activities measured on the microarray were dependent on ATP as very low activities were measured in absence of added ATP. The highest repair rates were reached with 1–2 mM ATP (data not shown).

Characterization of the excision/synthesis reaction

To further characterize the reaction that occurred at damaged plasmid sites on the slides, we performed the repair experiments in the simultaneous presence of two different nucleotides labelled with distinct dyes (dCTP-Cy3 and dGTP-Cy5) and with 2 mM

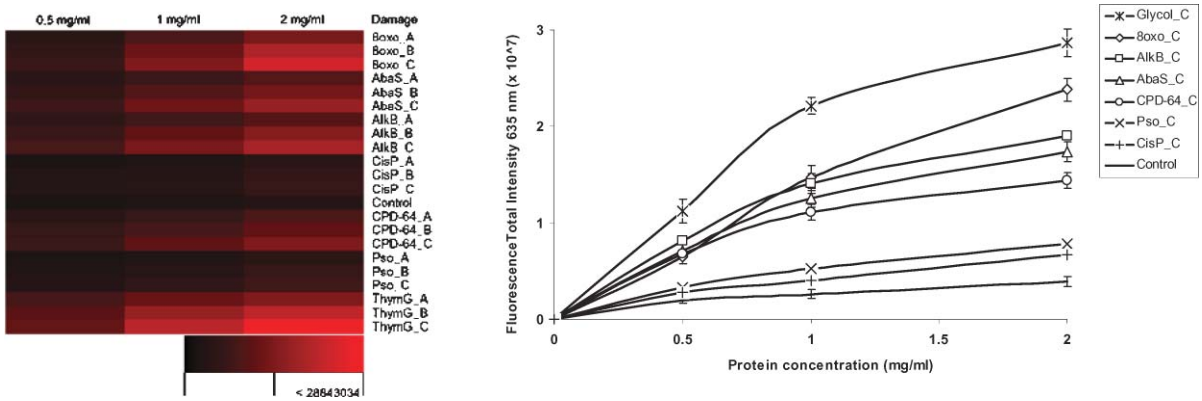

Fig. 3 Dependence of the repair signal on the amount of proteins. The assay was performed with 3 dilutions of HeLa nuclear extracts (0.5, 1 and 2 mg mL^{-1}). The colour map revealed that the signal was dependent on the amount of damage (damaged plasmid dilutions A, B and C) and on the protein content. Bright red corresponds to high fluorescence level (a). The curves represented the repair profiles of the C damage dilution (b).

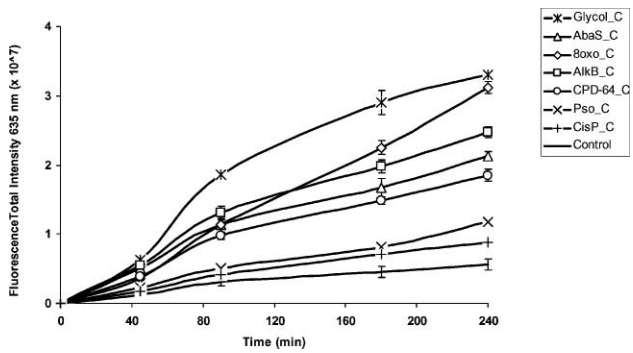

Fig. 4 Kinetics of the repair reaction performed on the plasmid microarray (45 min, 1 h 30, 3 h, 4 h). The assay was performed with HeLa nuclear extracts at 2 mg mL^{-1} and with an ATP concentration of 1 mM. The curves displayed corresponded to the repair kinetic of damaged plasmid C dilutions. The same kind of profile was obtained with plasmid dilution A and B, although with lower fluorescence intensity (data not shown).

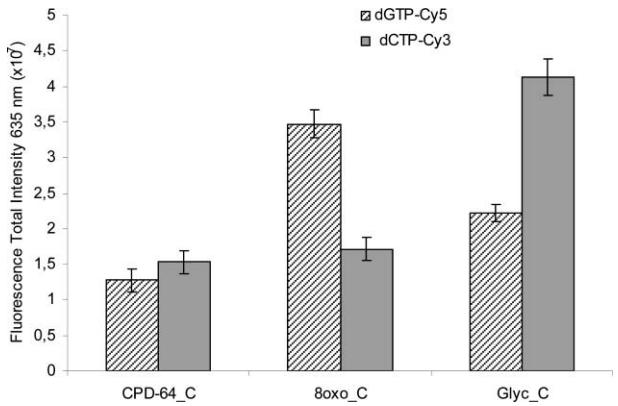

Fig. 5 Incorporation of dGTP-Cy5 (hatched bar) and dCTP-Cy3 (grey bar) by HeLa nuclear extracts at 2 mg mL^{-1} for 1 h. Fluorescent signal of the C damage dilution is reported for pCPD-64, p8oxo and pGlycol. Results showed the preferential incorporation of dGTP-Cy5 in place of 8-oxoGua and of dCTP-Cy3 in place of cytosine glycols, data consistent with BER of these lesions, whereas the incorporation ratio of both nucleotides was similar for CPD, lesions typically repaired by NER. Replicated experiments using a dye-swap strategy showed that there was no prominent dye effect (data not shown).

ATP. p8oxo showed the preferential incorporation of dGTP-Cy5 whereas pGlycol showed the preferential incorporation of dCTP-Cy3 (Fig. 5). These results demonstrated that the replacement of the base lesion 8-oxoGua by its normal counterpart guanine was prevalent in p8oxo plasmid and that cytosine glycols were preferentially replaced by the normal cytosine bases in pGlycol, as expected for lesions handled by BER. The incorporation rate of dCTP-Cy3 and dGTP-Cy5 was similar at plasmid sites containing lesions processed by NER which incorporates the different bases in the removed portion of DNA.

In order to characterize the DNA polymerase involved in the DNA synthesis step, we performed the assay in the presence of different concentrations of the polymerase ε and δ inhibitor aphidicolin (0–10 μg mL^{-1}). Aphidicolin-dependent inhibition of the ES signal demonstrated that in our *in vitro* assay DNA synthesis by replicative polymerases was predominant (data not shown).

Validation of the excision/synthesis assay using extracts from human XP cell lines

As a final validation of the assay, we tested the ES activities of nuclear extracts prepared from 2 XPC, 1 XPA, and 1 XPG cell lines. XPC protein is involved in the initial step of damage recognition; XPA encodes a protein involved in different key steps of the NER process, from damage recognition to incision of the damaged DNA and XPG gene encodes a nuclease.[6] Results were expressed as percentage of MRC5 ES capacity for the different lesions using the total fluorescence intensity. Marked impaired ES capacities were observed for all XP cell lines compared to normal MRC5 (Table 2). A striking feature was that repair of all types of lesions was modulated in XP cells. The ES phenotype was then analyzed 24 h after exposure to a very low dose of UVB at which ES capacities of normal cells were efficiently stimulated. Interestingly, results showed the inability of XPC cells to adapt their repair capacities following UVB exposure. The same feature was also observed for XPA cell extracts although to a lesser extend. This lack of significant response of the XP cells following UVB irradiation was observed toward any base lesion, whether repaired by NER or by BER (Fig. 6).

Table 2 Level of excision/synthesis capacities of different XP cell strains. The ES efficiency was calculated as a percentage of the value (total fluorescence intensity of damage dilutions A, B and C, minus total fluorescence intensity of pControl) obtained with normal control cells MRC5. The results were obtained after 2 h repair using 0.20 mg mL^{-1} of proteins

	pCPD-64	p8oxo	pAlkB	pAbaS	pGlycol
MRC5	100	100	100	100	100
AS1WT (XPC)	44 ± 2	39 ± 3	56 ± 2	62 ± 4	54 ± 2
GM16093 (XPC)	35 ± 2	27 ± 4	56 ± 2	69 ± 5	64 ± 4
XP12ROSV (XPA)	40 ± 2	41 ± 3	57 ± 2	61 ± 5	56 ± 3
GM14930 (XPG)	38 ± 2	41 ± 3	56 ± 2	74 ± 6	56 ± 3

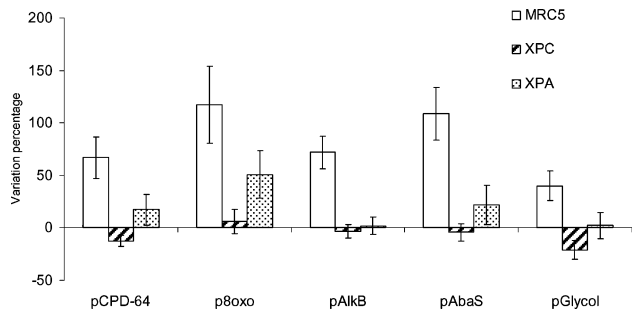

Fig. 6 Effect of UVB irradiation (5 J m^{-2}) on excision/synthesis capacities of MRC5, XPC and XPA cells. Extracts were prepared 24 h after the irradiation. Results are expressed as the variation in percentage of total fluorescence intensity (sum of fluorescence intensity of damaged plasmid dilutions A, B and C minus the value of pControl) calculated for each lesion between the irradiated and the non irradiated cells. Positive values revealed a stimulating effect of UVB irradiation on ES capacities of cells.

Measurement of excision/synthesis by PBMCs extracts

PBMCs isolated from 6 healthy volunteers were compared for their ability to perform the ES assay *in vitro*. Fluorescence incorporation by nuclear extracts was time-dependent and dependent on the amount of lesion except for donor 3 (S3) which showed extremely low ES capacity (Fig. 7). Each individual subject showed a specific repair phenotype. To illustrate this diversity we focused on 2 parameters that characterized ES capacity and can be used to differentiate the repair phenotypes of the different individuals: the total fluorescence intensity calculated as described in "Materials and methods" and the relative proportion of repair of the different DNA lesions. The values of these latter parameters are reported for the 60 min time point in Fig. 8a and Fig. 8b, respectively, where the reaction was time- and quantity of lesion-dependent. Results revealed large quantitative and qualitative differences between individuals.

Discussion

There is a strong interest in the development of DNA repair phenotyping assays and in their applications. Recently, an oligonucleotide cleavage assay revealed inter-individual variations in the repair of 8-oxoGua,[33] and a low repair of this lesion seems to correlate with an increased risk of lung cancer.[34] Methods used in these studies allowed the collection of valuable data but are not always easy to handle and only provide information about the repair of a single type of lesion. Taking advantage of miniaturized formats originally developed for genomic and proteomic studies, we have conceived a new enzymatic assay for the phenotyping of DNA repair activities contained in cell-free extracts. The development of this damaged plasmid microarray required optimization of all the steps necessary for its production and represented a technological challenge.

The aim was to measure major DNA repair enzyme activities and this was addressed through the repair of a subset of emblematic DNA lesions. Lesions were created in closed-circular plasmids by selected physical treatments and chemical agents. Damaging agents were carefully selected to generate specific DNA lesions without creating strand-breaks that would lead to unspecific repair signal. The repair efficiency and rate varied with the nature of the lesions. The number of lesions per plasmid was quantified by HPLC coupled to tandem mass spectrometry (except for psoralen adducts and Cg) and adjusted to obtain balanced repair signals using HeLa nuclear extracts as a reference (Table 1, Fig. 3 and Fig. 4). BER and NER are multi-step processes; repair curves obtained for the different substrates (Fig. 3 and Fig. 4) could reflect the diversity of the enzymes involved and the complexity of their interactions.[35] Fluorescent repair signals depended on protein concentration, time and ATP, the latter being an important component of BER and NER pathways. Finally, aphidicolin and dNTP-dyes experiments provided insights into the mechanisms involved in repair.

To further validate the assay, reactions were performed with nuclear extracts of fibroblast cell lines established from XP patients. For the first time, repair of different lesions was measured simultaneously, within a context of competitive damage recognition, using a highly sensitive normalized assay. As partially demonstrated a few years ago by Reardon *et al*[36] and more recently by D'Errico *et al*,[37] we showed that XPC is indeed involved in the repair of bulky lesions (induced by UVC) but also in the repair of oxidative base lesions. Hence we confirmed here that a wider role than repair of bulky damage can be attributed to this protein. Considering our results, the same conclusion could apply for XPA and XPG proteins. The ES rates we obtained using XPA extracts were higher than some published data for these cells, where limited incision was observed for UV-induced lesions.[38] Nevertheless, they were close to the one determined using the same kind of experiments on oxidative damage.[39] An explanation to these discrepancies could be, apart from the fact that our assay was adjusted to be very sensitive, that whole cell extracts were usually used while our assay involved nuclear extracts. A recently published paper[40] could bring new interesting clues regarding these apparently contradictory results. It showed that in unirradiated cells, XPA is present in the cytoplasm and translocated into the nucleus as a specific response to UV irradiation. Indeed, consequences of redistribution of proteins following UV irradiation cannot be observed when whole cell extracts are used. The nuclear and cytoplasmic compartments contain different repair proteins[41] that probably all participate in the repair process when whole cell extracts are used. DNA repair assays would gain from extensive comprehension of these discrepancies and harmonization of the protocols used to prepare cell-free extracts.

Interestingly, measurement of ES capacities of cells in response to UVB irradiation clearly discriminated XP from

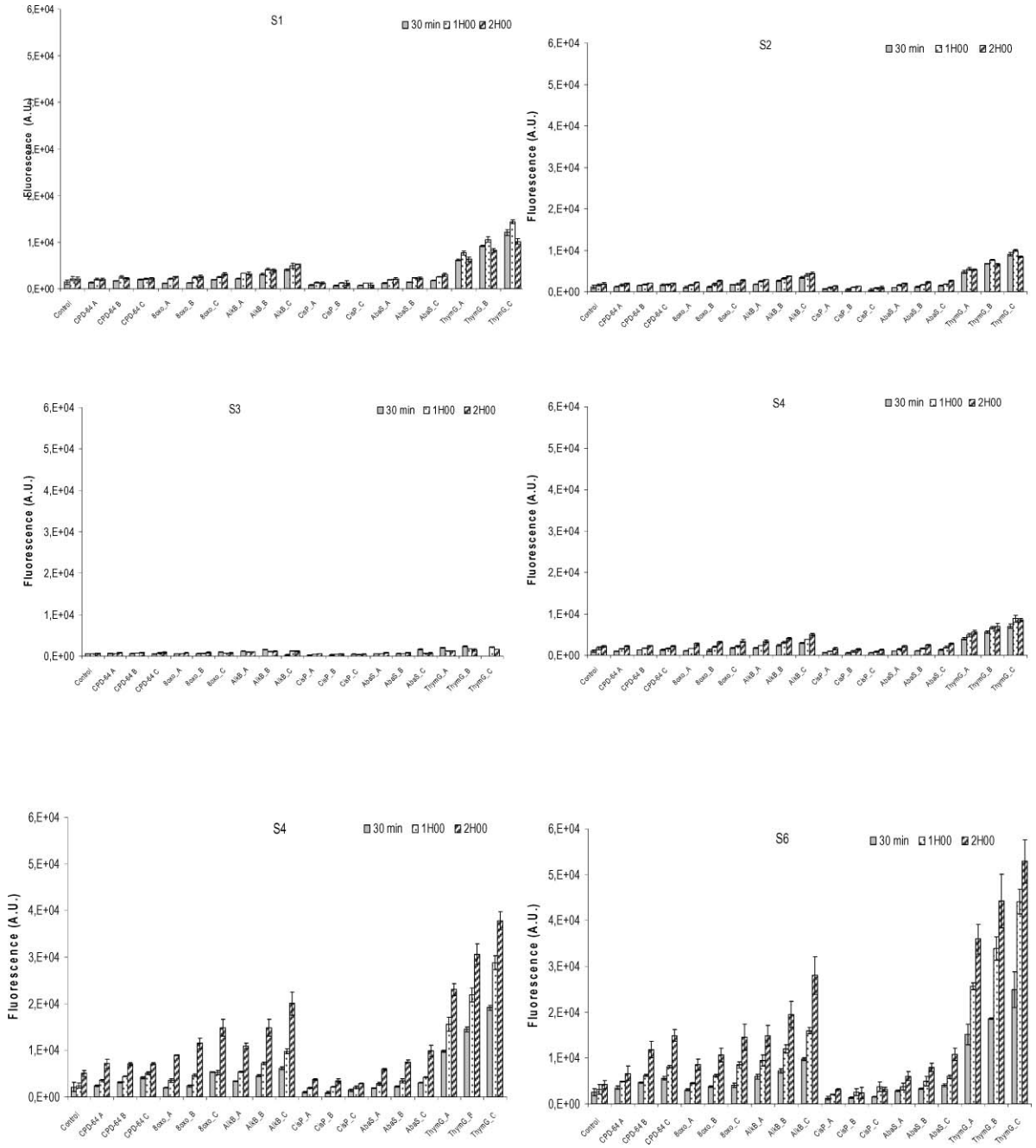

Fig. 7 Kinetic of the excision/synthesis reaction of the PBMCs from 6 different donors. The repair kinetic is shown for 30 min, 1 h and 2 h.

normal cells. Moreover, impaired response of XPC and XPA cells after UVB exposure correlated with the observed cytotoxicity at this dose (see Materials and methods) and with the rate of UV-induced UDS generally observed for these groups of complementation.[42]

We were able to directly measure excision/synthesis activities in PBMCs, without the need to culture, stimulate or transfect them, necessary steps of the host cell reactivation assay.[14] This constitutes a significant advantage for population-based studies. As observed by others,[44] the range of repair activities measured between individuals was quite broad; the two parameters we have selected will be very useful to stratify subjects for epidemiological studies in relation to DNA repair capacities.

The damaged plasmid microarray assay presented here is a powerful test that opens new opportunities to investigate DNA repair. It is fast, easy to perform and there is no restriction in terms of cell type that can be used. Clustering of data, initially developed to determine gene expression profile similarity, might be advantageously used to identify co-regulated proteins or proteins involved in the same pathways. It can be used to complement the information gained through our previously described assay that allows quantification of glycosylase activities in cell lysates.[44] Repair profiling may be obtained with extract prepared from less than 10^6 cells (data not shown). Potential applications include analyzing repair under different physiological conditions, getting insights into consequences

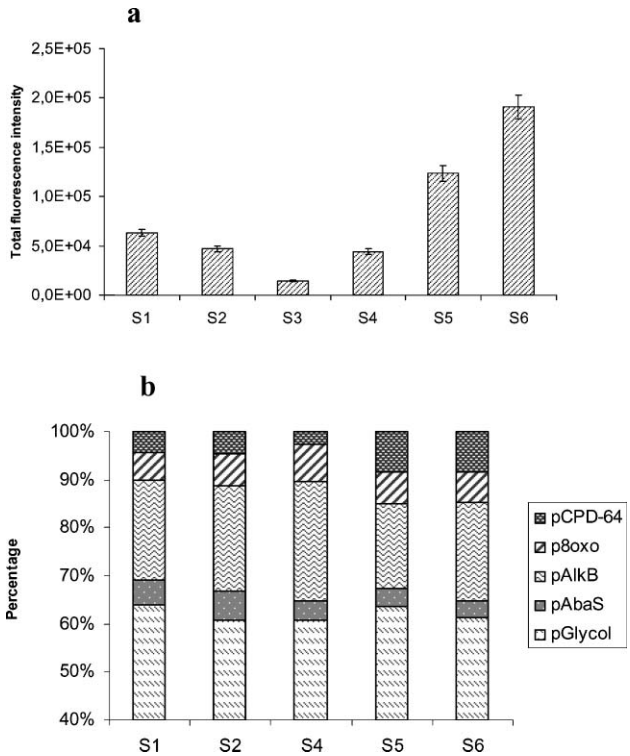

Fig. 8 Characterization of DNA excision/synthesis activities of PBMCs from the different donors. Total repair fluorescence intensity was calculated as described in "Materials and methods" (a). Contribution in percentage to the total fluorescence intensity of the repair activity toward each lesion for each donor (b).

of repair gene polymorphism at a functional level, detecting individuals with defective DNA repair and at high risk for cancer and identifying patients prone to side effects or resistance to antitumor treatments. A high-throughput version of the assay could help identify toxic repair inhibitors and help future drugs target specific repair pathways.[45]

Acknowledgements

We warmly thank Dr Jean Cadet for the scientific environment he has built. We are also thankful to Didier Grunwald for his help regarding confocal microscopy experiments. This work was supported in part by the Greiter foundation and in part by the COMICS STREP European project. We acknowledge the transversal programme "Technologies for health" of the CEA for its financial support. We thank Dr Serge Candéias for his contribution to the redaction of the manuscript.

References

1 R. E. Rasmussen and R. B. Painter, Evidence for repair of ultraviolet damaged deoxyribonucleic acid in cultured mammalian cells, *Nature*, 1964, **203**, 1360–1362.
2 J. E. Cleaver, Defective repair replication of DNA in xeroderma pigmentosum, *Nature*, 1968, **218**, 652–656.
3 J. R. Mitchell, J. H. Hoeijmakers and L. J. Niedernhofer, Divide and conquer: nucleotide excision repair battles cancer and ageing, *Curr. Opin. Cell Biol.*, 2003, **15**, 232–240.
4 D. B. Lombard, *et al.*, DNA repair, genome stability, and aging, *Cell*, 2005, **120**, 497–512.
5 P. C. Hanawalt, J. M. Ford and D. R. Lloyd, Functional characterization of global genomic DNA repair and its implications for cancer, *Mutat. Res.*, 2003, **544**, 107–114.
6 A. R. Lehmann, DNA repair-deficient diseases, xeroderma pigmentosum, Cockayne syndrome and trichothiodystrophy, *Biochimie*, 2003, **85**, 1101–1111.
7 J. Ding, Z. H. Miao, L. H. Meng and M. Y. Geng, Emerging cancer therapeutic opportunities target DNA-repair systems, *Trends Pharmacol. Sci.*, 2006, **27**, 338–344.
8 R. D. Wood, Nucleotide excision repair in mammalian cells, *J. Biol. Chem.*, 1997, **272**, 23465–23468.
9 H. E. Krokan, H. Nilsen, F. Skorpen, M. Otterlei and G. Slupphaug, Base excision repair of DNA in mammalian cells, *FEBS Lett.*, 2000, **476**, 73–77.
10 M. Dusinska, Z. Dzupinkova, L. Wsolova, V. Harrington and A. R. Collins, Possible involvement of XPA in repair of oxidative DNA damage deduced from analysis of damage, repair and genotype in a human population study, *Mutagenesis*, 2006, **21**, 205–211.
11 D. F. Lee, R. Drouin, P. Pitsikas and A. J. Rainbow, Detection of an involvement of the human mismatch repair genes hMLH1 and hMSH2 in nucleotide excision repair is dependent on UVC fluence to cells, *Cancer Res.*, 2004, **64**, 3865–3870.
12 A. Mazurek, M. Berardini and R. Fishel, Activation of human MutS homologs by 8-oxo-guanine DNA damage, *J. Biol. Chem.*, 2002, **277**, 8260–8266.
13 A. R. Collins, The comet assay for DNA damage and repair: principles, applications, and limitations, *Mol. Biotechnol.*, 2004, **26**, 249–261.
14 Y. Qiao, *et al*, Rapid assessment of repair of ultraviolet DNA damage with a modified host-cell reactivation assay using a luciferase reporter gene and correlation with polymorphisms of DNA repair genes in normal human lymphocytes, *Mutat. Res.*, 2002, **509**, 165–174.
15 C. D'Ham, A. Romieu, M. Jaquinod, D. Gasparutto and J. Cadet, Excision of 5,6-dihydroxy-5,6-dihydrothymine, 5,6-dihydrothymine, and 5-hydroxycytosine from defined sequence oligonucleotides by Escherichia coli endonuclease III and Fpg proteins: kinetic and mechanistic aspects, *Biochemistry*, 1999, **38**, 3335–3344.
16 V. Kumar, *et al.*, Riboflavin and UV-light based pathogen reduction: extent and consequence of DNA damage at the molecular level, *Photochem. Photobiol.*, 2004, **80**, 15–21.
17 A. Lambrinakos, K. E. Humphrey, J. J. Babon, T. P. Ellis and R. G. Cotton, Reactivity of potassium permanganate and tetraethylammonium chloride with mismatched bases and a simple mutation detection protocol, *Nucleic Acids Res.*, 1999, **27**, 1866–1874.
18 A. P. Loureiro, P. Di Mascio, O. F. Gomes and M. H. Medeiros, trans,trans-2,4-decadienal-induced 1,N(2)-etheno-2′-deoxyguanosine adduct formation, *Chem. Res. Toxicol.*, 2000, **13**, 601–609.
19 T. Buterin, *et al.*, Trapping of DNA nucleotide excision repair factors by non repairable carcinogen adducts, *Cancer Res.*, 2002, **62**, 4229–35.
20 D. Gunz, M. T. Hess and H. Naegeli, Recognition of DNA adducts by human nucleotide excision repair. Evidence for a thermodynamic probing mechanism, *J. Biol. Chem.*, 1996, **271**, 25089–25098.
21 K. L. Baxter-Gabbard, A simple method for the large-scale preparation of sucrose gradients, *FEBS Lett.*, 1972, **20**, 117–119.
22 S. Mouret, *et al.*, From the Cover: Cyclobutane pyrimidine dimers are predominant DNA lesions in whole human skin exposed to UVA radiation, *Proc. Natl. Acad. Sci. U. S. A.*, 2006, **103**, 13765–13770.
23 S. Courdavault, *et al.*, Larger yield of cyclobutane dimers than 8-oxo-7,8-dihydroguanine in the DNA of UVA-irradiated human skin cells, *Mutat. Res.*, 2004, **556**, 135–142.
24 F. Hazane, S. Sauvaigo, T. Douki, A. Favier and J. C. Béani, Age-dependent DNA repair and cell cycle distribution of human skin fibroblasts in response to UVA irradiation, *J. Photochem. Photobiol., B*, 2006, **82**, 214–223.
25 J. D. Dignam, R. M. Lebovitz and R. G. Roeder, Accurate transcription initiation by RNA polymerase II in a soluble extract from isolated mammalian nuclei, *Nucleic Acids Res.*, 1983, **11**, 1475–1489.
26 B. Salles and C. Provot, In vitro chemiluminescence assay to measure excision repair in cell extracts, *Methods Mol. Biol.*, 1999, **113**, 393–401.

27 R. D. Wood, P. Robins and T. Lindahl, Complementation of the xeroderma pigmentosum DNA repair defect in cell-free extracts, *Cell*, 1988, **53**, 97–106.
28 R. D. Wood, DNA repair in eukaryotes, *Annu. Rev. Biochem.*, 1996, **65**, 135–167.
29 M. Kartalou and J. M. Essigmann, Recognition of cisplatin adducts by cellular proteins, *Mutat. Res.*, 2001, **478**, 1–21.
30 J. Llano, J. Raber and L. Erikson, Theoretical study of phototoxic reactions of psoralens, *Photochem. Photobiol.*, 2003, **153**, 235–243.
31 V. M. Carvalho, *et al.*, Formation of 1,N6-etheno-2′-deoxyadenosine adducts by trans, trans-2, 4-Decadienal, *Chem. Res. Toxicol.*, 1998, **11**, 1042–1047.
32 A. Lambrinakos, K. E. Humphrey, J. J. Babon, T. P. Ellis and R. G. Cotton, Reactivity of potassium permanganate and tetraethylammonium chloride with mismatched bases and a simple mutation detection protocol, *Nucleic Acids Res.*, 1999, **27**, 1866–1874.
33 T. Paz-Elizur, *et al.*, Development of an enzymatic DNA repair assay for molecular epidemiology studies: distribution of OGG activity in healthy individuals, *DNA Repair*, 2007, **6**, 45–60.
34 T. Paz-Elizur, *et al.*, DNA repair activity for oxidative damage and risk of lung cancer, *J. Natl. Cancer Inst.*, 2003, **95**, 1312–1319.
35 S. L. Allinson, K. M. Sleeth, G. E. Matthewman and G. L. Dianov, Orchestration of base excision repair by controlling the rates of enzymatic activities, *DNA Repair*, 2004, **3**, 23–31.
36 J. T. Reardon, T. Bessho, H. C. Kung, P. H. Bolton and A. Sancar, In vitro repair of oxidative DNA damage by human nucleotide excision repair system: Possible explanation for neurodegeneration in Xeroderma pigmentosum patients, *Proc. Natl. Acad. Sci. U. S. A.*, 1997, **94**, 9463–9468.
37 M. D'Errico *et al.*, New functions of XPC in the protection of human skin cells from oxidative damage, *EMBO J.*, 2006, **25**, 4305–4315.
38 P. Robins, C. J. Jones, M. Biggerstaff, T. Lindahl and R. D. Wood, Complementation of DNA repair in xeroderma pigmentosum group A cell extracts by a protein with affinity for damaged DNA, *EMBO J.*, 1991, **10**, 3913–3921.
39 L. J. Lipinski, *et al.*, Repair of oxidative DNA base lesions induced by fluorescent light is defective in xeroderma pigmentosum group A cells, *Nucleic Acids Res.*, 1999, **27**, 3153–3158.
40 X. Wu, S. M. Shell, Y. Liu and Y. Zou, ATM-dependent, checkpoint modulates XPA nuclear import in response to UV irradiation, *EMBO J.*, 2007, **26**, 757–764.
41 V. Tembe and B. R. Henderson, Protein trafficking in response to DNA damage, *Cell. Signalling*, 2007, **19**, 1113–1120.
42 K. H. Kraemer and Hanoch S. Xeroderma, pigmentosum, *Clinics Dermatol.*, 1985, **3**, 33–69.
43 I. Gaivao, A. Piasek, S. Shaposhnikov and A. R. Collins, Comet-assay based methods for measuring DNA repair in vitro; estimates of inter- and intra-individual variation, *Cell Biol. Toxicol.*, 2007.
44 V. Guerniou, *et al.*, Repair of oxidative damage of thymine by HeLa whole-cell extracts: simultaneous analysis using a microsupport and comparison with traditional PAGE analysis, *Biochimie*, 2005, **87**, 151–159.
45 G. Damia and M. D'Incalci, Targeting DNA repair as a promising approach in cancer therapy, *Eur. J. Cancer*, 2007, **43**, 1791–1801.

